Cyclical Interactions between Two Outer Doublet Microtubules in Split Flagellar Axonemes

Susumu Aoyama* and Ritsu Kamiya*†
*Department of Biological Sciences, Graduate School of Science, University of Tokyo, Tokyo, Japan; and †CREST, Japan Science and Technology Corporation, Kawaguchi, Japan

ABSTRACT The beating of cilia and flagella is based on the localized sliding between adjacent outer doublet microtubules; however, the mechanism that produces oscillatory bending is unclear. To elucidate this mechanism, we examined the behavior of frayed axonemes of *Chlamydomonas* by using high-speed video recording. A pair of doublet microtubules frequently displayed association and dissociation cycles in the presence of ATP. In many instances, the dissociation of two microtubules was not accompanied by noticeable bending, suggesting that the dynein-microtubule interaction is not necessarily regulated by the microtubule curvature. On rare occasions, association and dissociation occurred simultaneously in the same interacting pair, resulting in a tip-directed movement of a stretch of gap between the pair. Based on these observations, we propose a model for cyclical bend propagation in the axoneme.

INTRODUCTION

Cilia and flagella are cell organelles for motility and are conserved among a variety of eukaryotic organisms. They produce remarkably rapid and regular bending waves through a mechanism that involves dynein-driven sliding between outer doublet microtubules (1). At this time, the fundamental question is the mechanism by which the microtubule sliding is organized into regular oscillatory bending movements. A number of models have been proposed based on assumption of certain feedback mechanisms wherein local sliding between microtubules is regulated by the axonemal curvature (2–7). For example, the ''geometric clutch'' model (6,7) proposes that transverse forces (t-forces) that act on the outer doublet microtubules regulate the activity of dynein to produce axonemal beating. The t-force acts to pry the two doublets apart in an active bend and pushes them together where an axoneme is passively bent, thus switching on and off the dynein activity. Computer simulation based on this model has been shown to reproduce essential features of cilia and flagella beating (6). Apart from computer modeling; however, little experimental evidence has been presented for the curvature-controlled feedback mechanism. In one of the few experimental studies, the sliding direction of doublet bundles in proteolyzed axonemes has been shown to reverse when the bundle is artificially bent (8). This finding could be taken as evidence for the curvature-controlled regulation of dynein activity. However, it is not clear whether microtubule curvature itself is the key factor that controls dynein activity, or whether some mechanical perturbation on dyneins located outside the bend is important. Therefore, the curvature-controlled feedback mechanism for flagellar beating has not been firmly established.

Although ciliary and flagellar axonemes usually have the so-called ''9 + 2'' structure composed of nine outer doublet microtubules and a pair of central microtubules, various organisms have cilia and flagella that lack the central-pair microtubules; for example, the flagella of eel sperm (9,10), the flagella of diatom gametes (11), and the nodal cilia in mouse embryos (12). *Chlamydomonas* flagella have a typical ''9 + 2'' organization, and mutants lacking the central pair or radial spokes are usually nonmotile (13,14). However, the mutant flagella recover the ability to beat when certain mutations are introduced into dynein or the dynein regulatory complex (DRC), a multiprotein complex postulated to regulate dynein activity (15–19). Furthermore, isolated mutant axonemes lacking the central pair or radial spokes can vigorously beat in certain nonphysiological solutions (20–22). These observations indicate that in *Chlamydomonas* flagella also, the central-pair microtubules are not essential for beating, suggesting that the essence of axonemal beating mechanism is contained in the nine outer doublet microtubules and associated structures.

In this study, to understand the essential features of the interaction between the outer doublets, we examined the behavior of a minimal functional unit of the axoneme, i.e., a pair of outer doublets. Using spontaneously frayed axonemes, experiments were previously performed in our laboratory to observe the behavior of structurally reduced axonemes. These studies have led to the findings that bundles of several doublet microtubules can propagate bending waves (23), and a pair of outer doublets can undergo cyclical association/dissociation interaction (24). However, these findings are based on rare observations and have not been quantitatively examined. For example, the ATP concentration in these experiments was unknown because the observations were made after a prolonged incubation in the reactivation solution without an ATP-regeneration system.

Submitted June 2, 2005, and accepted for publication August 3, 2005.

Address reprint requests to Ritsu Kamiya, Dept. of Biological Sciences, Graduate School of Science, University of Tokyo, 7-3-1 Hongo, Bunkyo-ku, Tokyo 113-0033, Japan. Tel.: 81-3-5841-4426; Fax: 81-3-5841-4632; E-mail: kamiyar@biol.s.u-tokyo.ac.jp.

0006-3495/05/11/3261/08 $2.00

doi: 10.1529/biophysj.105.067876

In addition, use of an ordinary video camera did not permit observation of fast movements. In this study, by using an efficient method to disintegrate axonemes along with high-speed video recording, we could clearly observe the cyclical movements in many microtubule pairs under controlled conditions. These new observations have provided important information regarding the dynein-microtubule interaction in beating axonemes.

MATERIALS AND METHODS

Preparation of axonemes

Axonemes were prepared from wild-type *Chlamydomonas reinhardtii*, using the dibucaine method of Witman et al. (14). Isolated flagella were suspended in HMDEK (30 mM Hepes-KOH (pH 7.4), 5 mM $MgSO_4$, 1 mM DTT, 1 mM EGTA, and 50 mM CH_3COOK) and demembranated with 0.1% (v/v) Nonidet-P40 in HMDEK. The sample was kept in ice until use.

Induction of axonemal disintegration

A flow chamber (sample volume, ~20 μl) consisting of a coverslip and a glass slide was placed under a microscope. The axonemes were introduced into the chamber and allowed to attach to the glass surface. The sample was then perfused with a disintegration solution containing 0.2–0.5 μg/ml nagarse (Sigma Type XXVII protease, Sigma-Aldrich, Tokyo, Japan), 100 μM ATP in pCa8-HMDEKP (30 mM Hepes-KOH (pH 7.4), 5 mM $MgSO_4$, 1 mM DTT, 50 mM CH_3COOK, 1% polyethylene glycol (MW, 20,000), 5 mM EGTA, 1 mM EDTA, and 0.9 mM $CaCl_2$) and left for ~3 min. It was then perfused with a low ATP concentration solution (10 μM ATP in pCa8-HMDEKP). This step resulted in extensive splitting of the axoneme. The movements in the disintegrated axonemes were observed after the sample was perfused with a reactivation buffer (pCa8-HMDEKP containing a desired concentration of ATP). The concentration of nagarse and the duration of the protease treatment were adjusted while monitoring disintegration under the microscope. Some axonemes were partially disintegrated on perfusion with only low ATP concentration solution. When axonemes were reactivated at low ATP concentrations ($\leq$100 μM), 5 mM creatine phosphate and 70 units/ml of creatine kinase (Roche Diagnostics, Tokyo) were added to the solution to maintain the concentration of ATP at a constant level.

Observation and recording

The movements of frayed axonemes were observed using a BX50 microscope (Olympus, Tokyo, Japan) equipped with a dark field condenser, a 40$\times$ objective (numerical aperature = 0.85), and a 100 W mercury arc lamp. The images were recorded with a high-speed CCD video camera (HAS-200R, Ditect, Tokyo, Japan) operated at 200 frames/s. The images were stored in a personal computer.

RESULTS

Production of frayed axonemes

To efficiently disintegrate the axonemes, we used a method similar to that used for induction of sliding disintegration, i.e., treatment with ATP and protease (25). We selected nagarse as the protease because it has been shown to be effective in the induction of sliding disintegration in *Chlamydomonas* axonemes (26). When axonemal samples were perfused with the disintegration solution containing nagarse and ATP, many axonemes were split into individual outer doublets within 2–3 min (Fig. 1). In most axonemes, the outer doublets remained connected to each other at the base for >60 min. The central-pair microtubules, which could be clearly distinguished from the outer doublets by their helical appearances (27,28), usually detached and floated away from the axonemes soon after the protease perfusion was started.

Oscillatory movements displayed by a pair of outer doublets

Some microtubule bundles in the frayed axonemes displayed cyclical movements on perfusion with the reactivation solution containing ATP. In typical cases, two doublet microtubules connected at their proximal ends showed repeated association and dissociation at a frequency that depended on the ATP concentration (Fig. 2, see supplementary movie 1). The association between the two doublet microtubules began at the proximal portion. After the associated portion had advanced to a certain length, the two microtubules started to dissociate at the base. The gap formed between the pair increased as the dissociation front moved toward the distal end, until the two microtubules became dissociated over their entire lengths. These tubules again became associated at the base, thereby completing a cycle. When ATP concentration was >0.1 mM, most of the doublet pairs did not form a large bend; the dissociation started after the short stretches of microtubules associated at the base. When the ATP concentration was <10 μM, some doublet pairs formed a large bend (Fig. 3). Although no systematic assay was conducted on the effect of varied Ca^{2+} concentrations, similar phenomena were observed at both pCa 8 and pCa 4 (S. Aoyama and R. Kamiya, unpublished observation).

ATP-dependent propagation of association/dissociation waves

Fig. 4 shows the change in the positions at which association and dissociation occurred between the microtubule pair

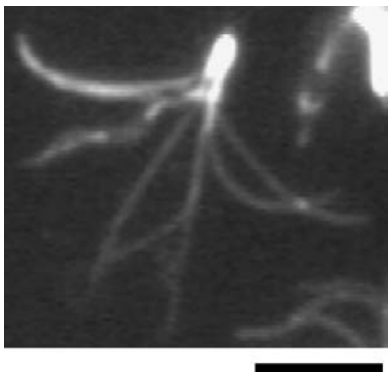

FIGURE 1 Split axoneme obtained by protease/ATP treatment. Video-recorded dark-field micrograph. The axonemes tend to split into single outer doublets and bundles, while their proximal ends remain connected. Bar, 5 μm.

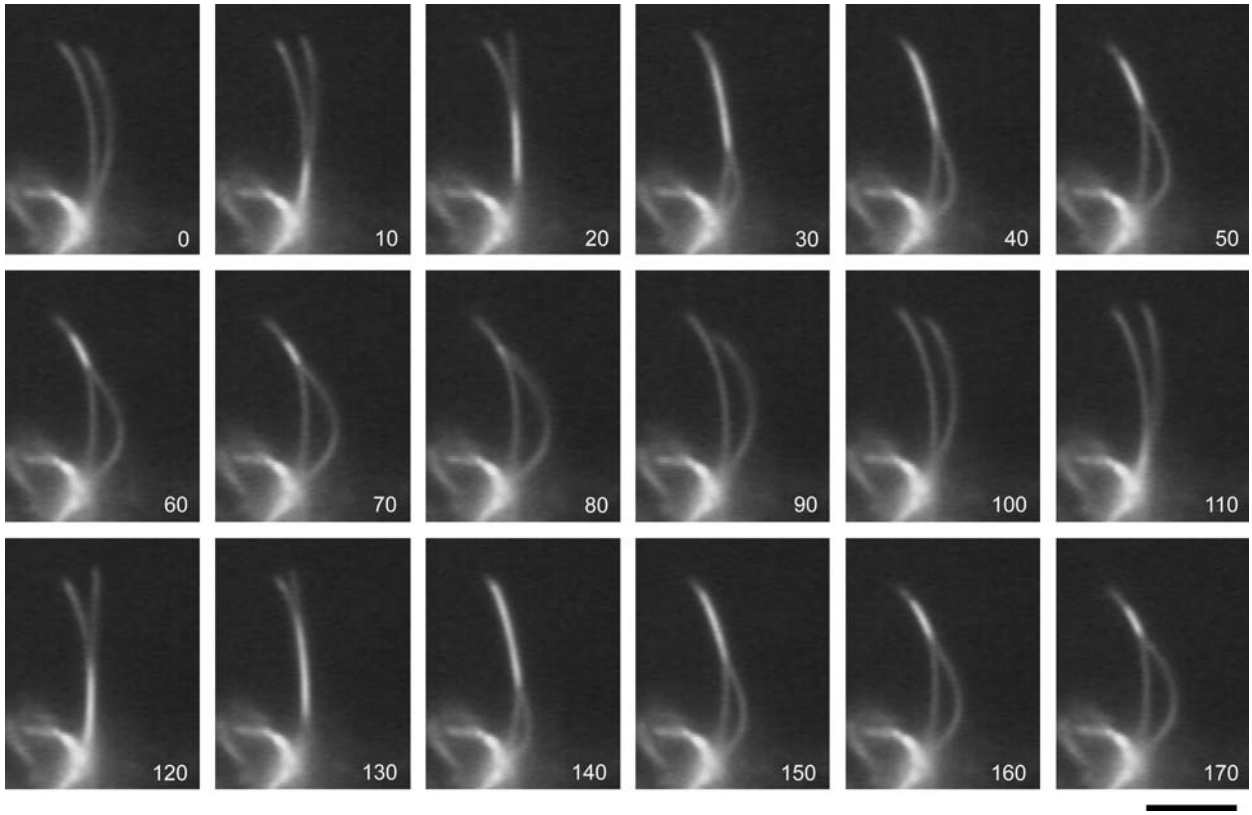

FIGURE 2 Cyclical interaction between a pair of outer doublet microtubules. A series of video frames taken every 10 ms (see supplementary movie 1 (fourfold slowed down)). The number in each frame shows the time in milliseconds. This pair repeats an association/dissociation cycle at ~9 Hz. Note that no significant bending occurs in the associated portion. ATP concentration, 500 μM. Bar, 5 μm.

shown in Fig. 2. Both the positions were measured along the microtubule that was positioned outside the arch. Immediately after their complete separation, the two microtubules again associated at the base. The front end of the associated portion (association point) then advanced toward the distal end at a fairly constant velocity (*open circles*; *curve 1*). After the association point had advanced to a certain length, the basal portion started to dissociate. Initially, the front end of the dissociated portion (dissociation point) rapidly proceeded toward the tip; later, the movement became progressively slower (*solid circles*; *curve 2*). In these plots, the vertical difference between *curve 1* and *curve 2* at a given time represents the length of the associated portion, whereas the horizontal difference at a given position represents the

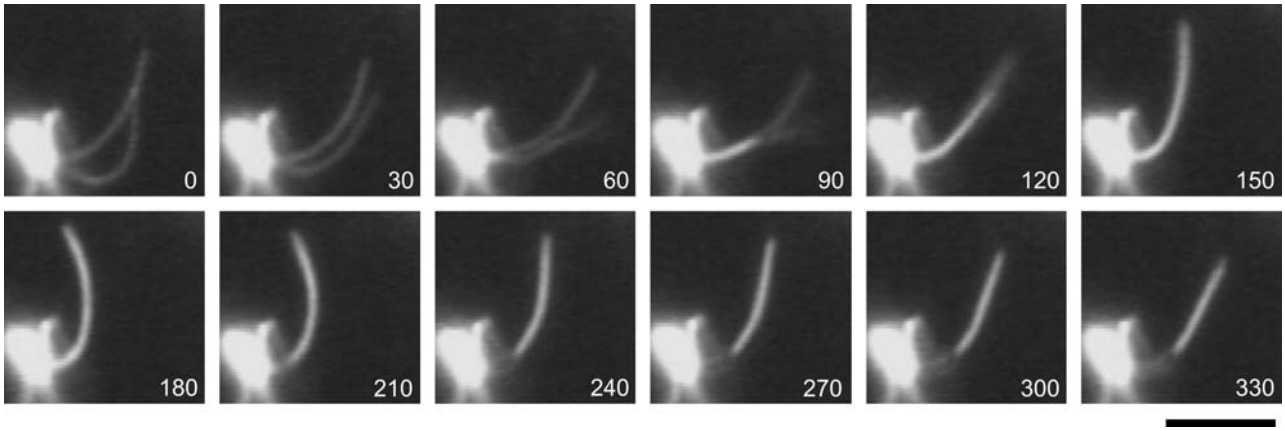

FIGURE 3 Doublet pair showing a bending movement. Video frames taken every 30 ms. This type of bending movement was frequently observed at lower ATP concentrations. ATP concentration, 5 μM. Bar, 5 μm.

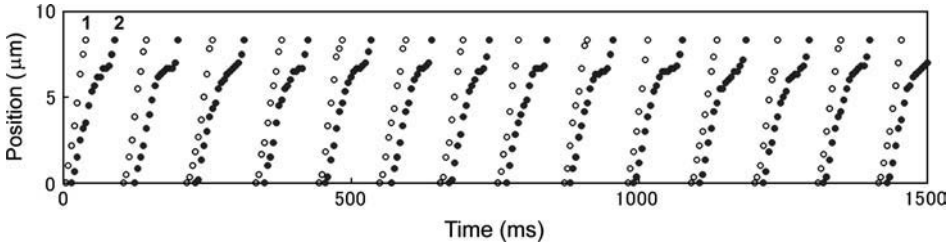

FIGURE 4 Change in the positions at which association (○; *curve 1*) and dissociation (●; *curve 2*) occurred between two doublet microtubules shown in Fig. 2. The doublet pair repeats association and dissociation at an almost constant frequency.

time for which the two microtubules remained associated. The slopes of these lines represent the velocities at which the association/dissociation points moved.

We measured the traveling speeds of the association and dissociation points at different ATP concentrations. As the velocity of the dissociation point, we selected the velocity in the early phase of dissociation, i.e., the highest velocity in the dissociation process. These velocities were found to be fairly constant among different pairs of outer doublets displaying oscillation under the same conditions. Measurements with eight axonemes at each ATP concentration revealed a clear difference in these velocities. The velocity of the dissociation point depended on the ATP concentration; this was consistent with the Michaelis-Menten kinetics. On the other hand, the velocity of the association point was independent of the ATP concentration (Fig. 5). With 1 mM ATP, the dissociation and association points moved at 250 μm/s and 400 μm/s, respectively. These speeds are of the same order as that of wave propagation in the axoneme ($\sim$600 μm/s at 1 mM ATP).

Other observations

Some pairs of microtubules showed movements that were different from the typical association/dissociation movement described above. These observations were rather rare, but provided important clues to the behavior of outer doublets in the axoneme.

One observation was the propagation of a ''gap'' between two doublets (Fig. 6, see supplementary movie 2). This movement was apparently generated by the simultaneous traveling of the dissociation and the association points.

Another interesting phenomenon was bend propagation in the bundles of outer doublets. When axonemes were maintained in the presence of low concentrations of ATP without any proteases, they often became frayed, similar to the observation in the previous studies (23,24). In these cases, most axonemes split into bundles of microtubules, each apparently containing 3–5 microtubules, rather than individual outer doublets. As reported previously, some microtubule bundles in these frayed axonemes propagated asymmetrical bending waves (Fig. 7). Thus, propagation of bending waves requires neither nine outer doublets nor a circular arrangement of microtubules.

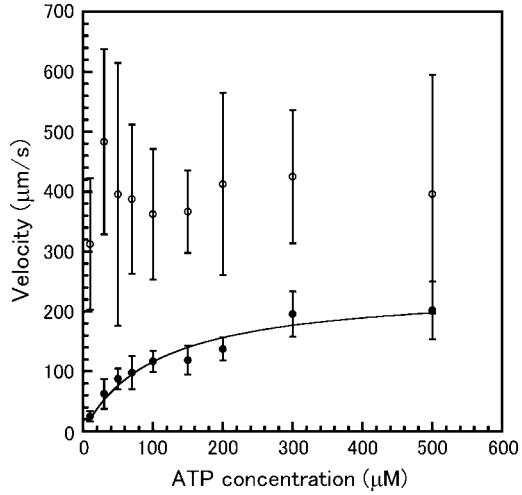

FIGURE 5 Maximal velocities of the association/dissociation front progression at different ATP concentrations. (○) The association front. (●) The dissociation front. (*Solid line*) Data for the dissociation front fitted to Michaelis-Menten kinetics with the following parameters: maximal velocity = 240 μm/s; Km = 107 μM. For each data point, the average and standard deviation (*error bars*) measured in eight samples are shown.

DISCUSSION

In this study, we developed a method to extensively disintegrate axonemes while maintaining the connection of outer doublets at the base. Using this method, we observed that pairs of doublet microtubules frequently display cyclical association/dissociation interaction. Although the general behavior of a microtubule pair in split axonemes is clearly different from that in intact axonemes, it probably reflects the fundamental properties of the mechanochemical dynein-microtubule interaction underlying the axonemal beating.

Phenomenological model

In most examples of association/dissociation interaction between doublet pairs that we observed, dissociation was apparently not triggered by a large curvature formed in the pair. This observation differs from the previous observation made by using axonemes that were spontaneously frayed in reactivation solutions (24); in the previous study, two outer doublets started to dissociate at the point where they formed a large bend, leading to the idea that the dynein-microtubule interaction is turned off when the microtubule curvature exceeds a certain critical value. However, this model cannot explain the observations made in this study.

Fig. 8 shows an interpretation of the experimental observation. After a pair of doublets associate for a certain length

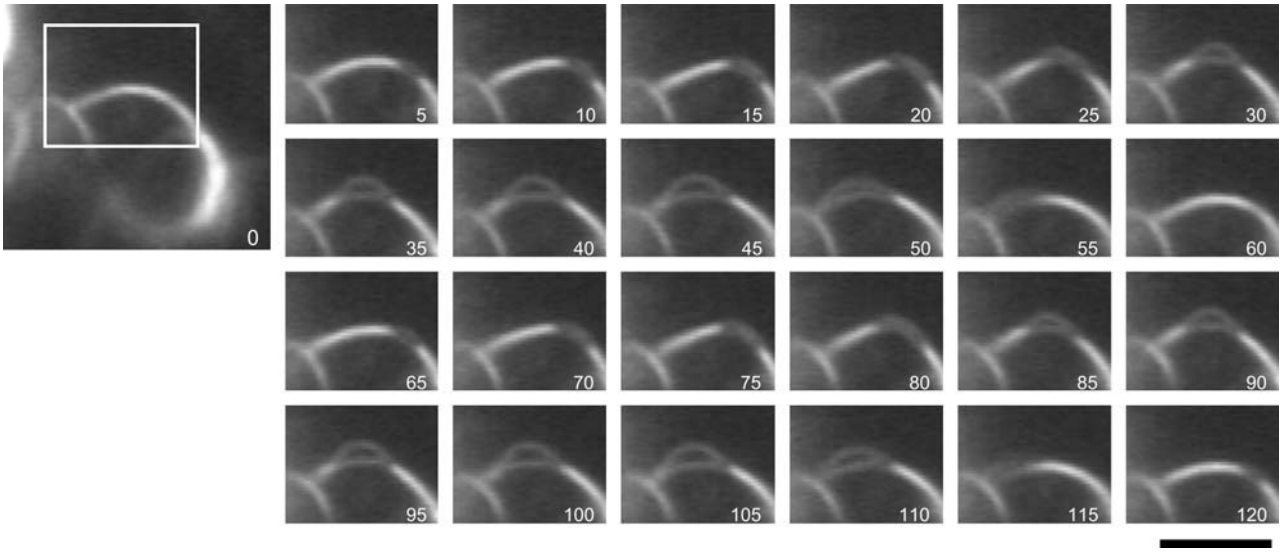

FIGURE 6 Pair of doublets displaying a distally traveling gap. Video frames taken every 5 ms (see supplementary movie 2 (fourfold slowed down)). ATP concentration, 100 μM. Bar, 5 μm.

(*a*), the basal portion starts to dissociate (*b*). The dissociated portion enlarges with time as the dissociation point travels distally (*c* and *d*), until the pair is completely separated from base to tip (*e*). The pair then start to associate with each other again at the base, with the association front moving toward the tip, returning to the first state (*a*). In this scheme, we assume that the outer doublet positioned on the outer side of the interacting pair (the right outer doublet in Fig. 8) bears dynein arms that interact with the other tubule, and these dyneins produce a shearing force, such that each dynein tends to move to the minus end (proximal end) of the adjacent microtubule (29). This force pulls the left tubule and pushes the right microtubule. Since dyneins can be regarded as independent force generators aligned in series, this shearing force must produce the largest bending moment at the base where the two doublet microtubules are presumed to be tightly connected. Here, we assume that the basal connection and microtubules have finite elasticity, and that the large bending moment results in distortion of dynein, which decreases the dynein-microtubule binding force. The force exerted by the row of dyneins in an interacting microtubule pair would therefore result in the dissociation of the pair at the base. Once a segment of a pair is dissociated, the dissociated portion cannot immediately reassociate because the relative sliding

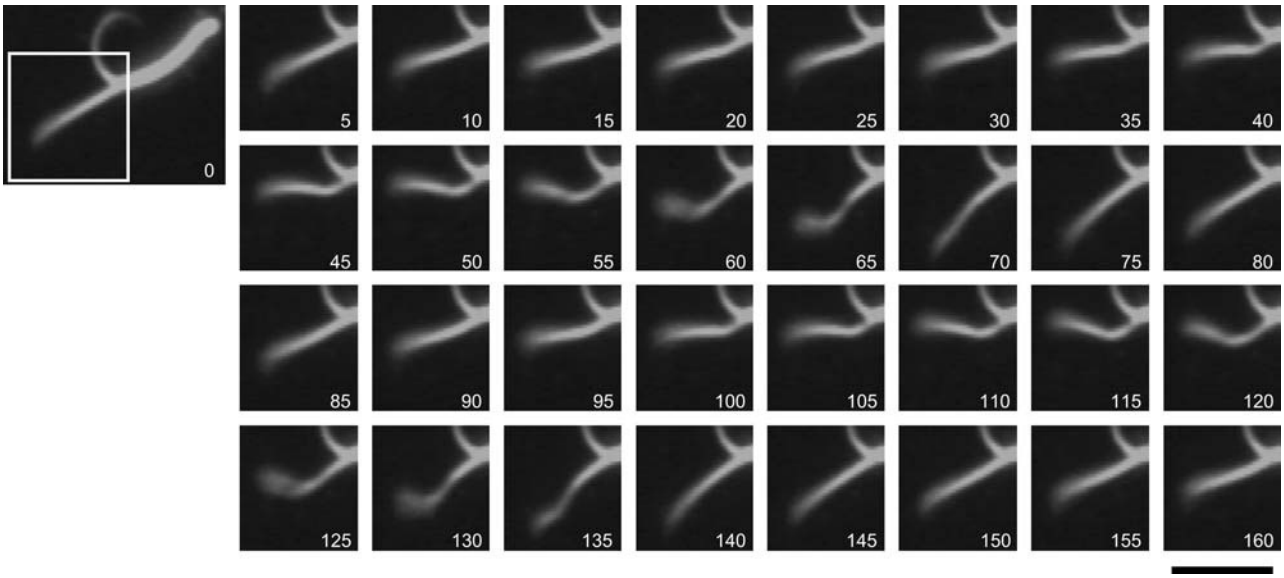

FIGURE 7 Bend propagation in a microtubule bundle in a split axoneme. One of the two microtubule bundles in a split axoneme (*left photo*) is propagating a bend, as seen in the sequential photos shown right. Video frames taken every 5 ms. ATP 100 μM. Bar, 5 μm.

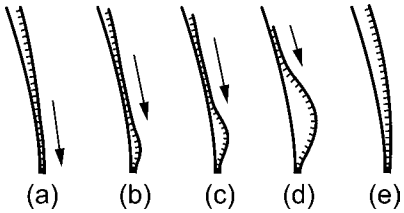

FIGURE 8 Model of the association/dissociation movement displayed by a doublet pair. (*a*) When two outer doublet microtubules are associated for a certain length, dynein (depicted by small projections on the right microtubule) generates sliding force. (*b*) The large bending moment at the base results in dissociation of the microtubules. (*c* and *d*) The dissociated portion spreads as the dissociation front moves toward the tip. (*e*) After complete dissociation, the two outer doublets start to reassociate at the base. The associated portion spreads as the association front moves toward the tip.

between the two microtubules causes one tubule (the tubule positioned on the outer side) to loop out. Hence, this dissociation process usually continues until the two microtubules are dissociated along their entire lengths. After complete dissociation, the two microtubules can readily reassociate at the base, where they are in close apposition.

The above interpretation is similar to the model proposed by Kamiya and Okagaki (24) to explain the cyclical bending interaction in a doublet pair or to the geometric clutch model presented by Lindemann (6) to explain the mechanism of flagellar oscillation. However, this model significantly differs from these models. That is, we assume that the dynein-microtubule interaction is directly turned off by the force acting on dynein cross-bridges, rather than by the increased curvature of microtubules. The oscillatory interaction between doublet pairs in the absence of bending is reminiscent of the high-frequency oscillation in the axoneme that also occurs without bending (30–32). Several pieces of evidence from these studies have indicated that outer doublets undergo back-and-forth oscillation through mechanical interaction between dynein and an axonemal elastic component and have led to the hypothesis that dynein force production is turned off by the force produced by dynein itself (31). This hypothesis is essentially the same as the assumption employed in this study.

Relationship with dynein kinetics

Our experiments showed that the dissociation rate between the two microtubules depended on the ATP concentration, whereas the association rate did not (Fig. 5). It is likely that the dissociation rate depends on the ATP concentration because each dynein molecule engaged in force production is alternating between a strong-binding state and a weak-binding state in an ATP concentration-dependent manner. Since the strong binding state lasts for a short duration at higher ATP concentrations (33), less time is required at higher ATP concentrations to zip apart dynein cross-bridges at the dissociation point. This idea also explains our observation of curved doublet pairs frequently occurring at low ATP concentrations. Under these conditions, two microtubules probably associate for a greater time and length, resulting in a large interdoublet shear that is sufficient to cause the bending of the whole structure (Fig. 3). In contrast to the dissociation point, the progression rate of the association point did not depend on the ATP concentration. This implies that dyneins on the outer doublet, after having been separated from the adjacent outer doublet for a certain period of time, have already hydrolyzed ATP and assumed a kinetic state wherein they can readily associate with a microtubule when brought into contact with it.

Force required for doublet dissociation

The simplicity of the paired-outer-doublet system prompts us to consider its force balance, particularly when a single doublet is looping out, as shown in Fig. 8 *b*. Here, for simplicity, we regard the outer doublet as a straight elastic rod, although it is intrinsically slightly curved. When a rod of length L is slightly bent by forces that push both ends, the force F acting on one end is given by:

$$F = \pi^2 EI/L^2,$$

where EI is the flexural rigidity. When both ends are clamped and kept in line with the direction of the force, F becomes four times greater than the value obtained using this formula (34). This equation implies that a force larger than a certain critical value (the Euler force), defined by the length and flexural rigidity of the rod, can bend it. In this case, L, the looped-out portion of the doublet, increases with time.

The flexural rigidity of microtubules has been estimated using various methods. Thus far, the values reported ranges between 0.5×10^{-24} and $>20 \times 10^{-24}$ Nm^2, depending on the method of measurement and association with MAPs or taxol; MAPs increase the flexural rigidity of microtubules by a factor of ~4, whereas taxol reduces it by a factor of ~4 (35,36). The flexural rigidity of the outer doublet microtubules has been measured in sea urchin sperm flagella and reported to be in the range of 14–61 $\times 10^{-24}$ Nm^2 (37). Since the outer doublet microtubule is most likely associated with various binding proteins, and its cross-section dimension is approximately twice that of a singlet, we assume that its flexural rigidity is close to or higher than the largest measured value. Thus, we selected the value of 60×10^{-24} Nm^2.

If we further assume that the dynein cross-bridges dissociate over a length of 1 μm when the two doublet microtubules start to dissociate at the base (as in Fig. 8 *b*), then the force required to bend the dissociated microtubule segment is ~2.3 nN. Since the force produced by a single dynein head has been estimated to be 1–5 pN (38–40), and a 1-μm segment of an outer doublet contains ~200 dynein heads, this means that the bending requires the force production by 400–2000 dynein heads, corresponding to the interdoublet interaction over 2–10 μm. If we assume a shorter initial

dissociation length, the force required to bend the microtubule must increase. However, since the oscillatory movement that we observed frequently occurred with only a short stretch of an interacting microtubule pair, it is unlikely that a stronger force is necessary to induce doublet dissociation. Therefore, for the two microtubules to interact according to the scheme shown in Fig. 8, the two outer doublets must first dissociate for a fairly long length, for example, 1 μm, at the base. This requires that the dissociation of dynein cross-bridges occur in a cooperative fashion.

In the above discussion, we assumed that the flexural rigidity of an outer doublet is independent of its length. However, recent experiments have suggested that the flexural rigidity of a microtubule is variable with length, roughly proportional to L^2, although the reason for the length-dependency has not been entirely clear (35,41). If this is true, we can estimate that force production by only 2–40 dynein heads would be sufficient to bend a microtubule segment of any length.

Implications for flagellar beating mechanism

The key point of the above model is in the assumption that the dynein-microtubule interaction at the base is mechanically turned off by the sliding force produced by a group of dyneins positioned distally. Such properties of the dynein-microtubule interaction may also be important in the beating of intact axonemes. We occasionally encountered pairs of microtubules that displayed association and dissociation simultaneously, resulting in the propagation of a short split portion (Fig. 6). In these pairs, it is likely that the basal portions start reassociation before the dissociation wave has reached the tip. Now, if we assume that some loose or elastic links are present between the two microtubules and restrict their separation within a certain limit (for example, twice the normal spacing), then we can expect that such a split portion will form a bend instead of a large loop (Fig. 9). In other words, propagation of bending waves occurs in a pair of doublet microtubules. An important point in this model is that, similar to the above model of association/dissociation propagation, the sliding force between the two doublet microtubules is assumed to disrupt the proximal cross-bridges between dyneins and microtubules, in addition to producing sliding displacements in the distal portion of the pair. A previous study that measured the radial movement in the axoneme demonstrated that the axoneme exhibits a significant variation in diameter during its function (42). Thus, the mechanical separation of adjacent microtubules in the axoneme may possibly play an essential role in the beating mechanism (6,7,24). If a bend in an axoneme is actually produced by the separation of outer doublets, dyneins in the most strongly bent portion should be regarded as inactive.

The above simple model for bending wave propagation by two outer doublets has an obvious limitation. That is, it can explain the generation of a bend only in one direction. To explain the generation of principal and reverse bends in a single axoneme, we must postulate distinct pairs of outer doublets that are oppositely positioned and produce bends in opposite directions. The mechanism by which the oscillatory movements produced by these two opposing pairs of doublets are coupled with each other remains to be elucidated.

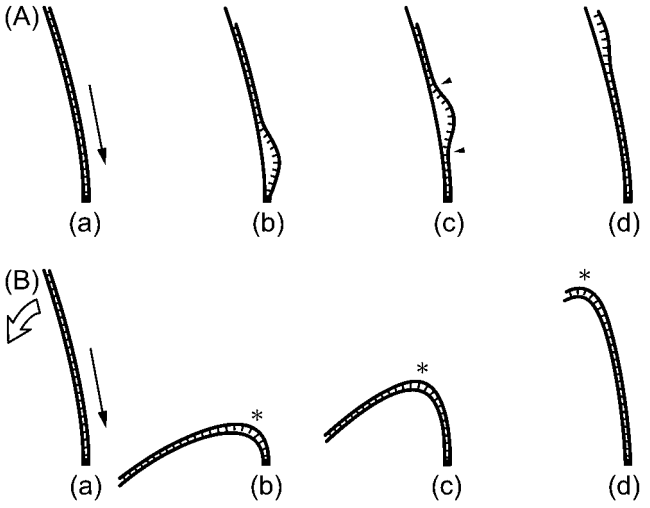

FIGURE 9 Model of wave propagation based on a ''gap'' movement. (*A*) Model for a traveling ''gap'' similar to that shown in Fig. 6. Simultaneous movements of the dissociation and association fronts (*arrowheads*) produce a distally traveling gap. (*B*) Model for bend propagation. If we assume that a gap is formed as in *A* but that the two outer doublets are connected by some loose structures, then interdoublet sliding will produce a bend (*asterisk*) that advances distally.

We have thus far shown that two outer doublets can undergo cyclical interactions without accompanying gross bending. However, we cannot rule out the possibility that the oscillatory movements we observed reflect some nonphysiological features of dynein-microtubule interaction, and that a curvature-controlled mechanism operates in the beating of intact axonemes that have nine circularly arranged outer doublets. The presence of the central-pair/radial spoke system in the axoneme may provide an additional mechanism for controlling dynein force generation based on axonemal curvature. These results, therefore, do not preclude curvature-controlled mechanisms; however, our results imply that curvature-independent mechanisms deserve serious consideration as well.

SUPPLEMENTARY MATERIAL

An online supplement to this article can be found by visiting BJ Online at http://www.biophysj.org.

This study has been supported by a grant from the Ministry of Education, Culture, Sports, Science and Technology of Japan.

REFERENCES

1. Gibbons, I. R. 1981. Cilia and flagella of eukaryotes. *J. Cell Biol.* 91:107s–124s.

2. Brokaw, C. J. 1971. Bend propagation by a sliding filament model for flagella. *J. Exp. Biol.* 55:289–304.

3. Brokaw, C. J. 1972. Flagellar movement: a sliding filament model. *Science.* 178:455–462.

4. Brokaw, C. J. 1982. Models for oscillation and bend propagation by flagella. *Symp. Soc. Exp. Biol.* 35:313–338.

5. Blum, J. J., and M. Hines. 1979. Biophysics of flagellar motility. *Q. Rev. Biophys.* 12:103–180.

6. Lindemann, C. B., and K. S. Kanous. 1997. A model for flagellar motility. *Int. Rev. Cytol.* 173:1–72.

7. Lindemann, C. B. 2003. Structural-functional relationships of the dynein, spokes, and central-pair projections predicted from an analysis of the forces acting within a flagellum. *Biophys. J.* 84:4115–4126.

8. Morita, Y., and C. Shingyoji. 2004. Effects of imposed bending on microtubule sliding in sperm flagella. *Curr. Biol.* 14:2113–2118.

9. Gibbons, B. H., B. Baccetti, and I. R. Gibbons. 1985. Live and reactivated motility in the 9+0 flagellum of *Anguilla* sperm. *Cell Motil.* 5:333–350.

10. Woolley, D. M. 1998. Studies on the eel sperm flagellum. 3. Vibratile motility and rotatory bending. *Cell Motil. Cytoskeleton.* 39:246–255.

11. Manton, I., K. Kowallik, and H. A. Stosch. 1970. Observations on the fine structure and development of the spindle at mitosis and meiosis in a marine centric diatom (*Lithodesmium undulatum*). 3. The later stages of meiosis I in male gametogenesis. *J. Cell Sci.* 6:131–157.

12. Nonaka, S., Y. Tanaka, Y. Okada, S. Takeda, A. Harada, Y. Kanai, M. Kido, and N. Hirokawa. 1998. Randomization of left-right asymmetry due to loss of nodal cilia generating leftward flow of extraembryonic fluid in mice lacking KIF3B motor protein. *Cell.* 95:829–837.

13. Warr, J. R., A. McVittie, J. T. Randall, and J. M. Hopkins. 1966. Genetic control of flagellar structure in *Chlamydomonas*. *Genet. Res.* 7:335–351.

14. Witman, G. B., J. Plummer, and G. Sander. 1978. *Chlamydomonas* flagellar mutants lacking radial spokes and central tubules. Structure, composition, and function of specific axonemal components. *J. Cell Biol.* 76:729–747.

15. Huang, B., Z. Ramanis, and D. J. Luck. 1982. Suppressor mutations in *Chlamydomonas* reveal a regulatory mechanism for flagellar function. *Cell.* 28:115–124.

16. Porter, M. E., J. Power, and S. K. Dutcher. 1992. Extragenic suppressors of paralyzed flagellar mutations in *Chlamydomonas reinhardtii* identify loci that alter the inner dynein arms. *J. Cell Biol.* 118:1163–1176.

17. Piperno, G., K. Mead, M. LeDizet, and A. Moscatelli. 1994. Mutations in the ''dynein regulatory complex'' alter the ATP-insensitive binding sites for inner arm dyneins in *Chlamydomonas* axonemes. *J. Cell Biol.* 125:1109–1117.

18. Gardner, L. C., E. O'Toole, C. A. Perrone, T. Giddings, and M. E. Porter. 1994. Components of a ''dynein regulatory complex'' are located at the junction between the radial spokes and the dynein arms in *Chlamydomonas* flagella. *J. Cell Biol.* 127:1311–1325.

19. Rupp, G., and M. E. Porter. 2003. A subunit of the dynein regulatory complex in *Chlamydomonas* is a homologue of a growth arrest-specific gene product. *J. Cell Biol.* 162:47–57.

20. Omoto, C. K., T. Yagi, E. Kurimoto, and R. Kamiya. 1996. Ability of paralyzed flagella mutants of *Chlamydomonas* to move. *Cell Motil. Cytoskeleton.* 33:88–94.

21. Wakabayashi, K., T. Yagi, and R. Kamiya. 1997. Ca^{2+}-dependent waveform conversion in the flagellar axoneme of *Chlamydomonas* mutants lacking the central-pair/radial spoke system. *Cell Motil. Cytoskeleton.* 38:22–28.

22. Yagi, T., and R. Kamiya. 2000. Vigorous beating of *Chlamydomonas* axonemes lacking central pair/radial spoke structures in the presence of salts and organic compounds. *Cell Motil. Cytoskeleton.* 46:190–199.

23. Nakamura, S., and R. Kamiya. 1978. Bending motion in split flagella of *Chlamydomonas*. *Cell Struct. Funct.* 3:141–144.

24. Kamiya, R., and T. Okagaki. 1986. Cyclical bending of two outer-doublet microtubules in frayed axonemes of *Chlamydomonas*. *Cell Motil. Cytoskeleton.* 6:580–585.

25. Summers, K. E., and I. R. Gibbons. 1971. Adenosine triphosphate-induced sliding of tubules in trypsin-treated flagella of sea-urchin sperm. *Proc. Natl. Acad. Sci. USA.* 68:3092–3096.

26. Okagaki, T., and R. Kamiya. 1986. Microtubule sliding in mutant *Chlamydomonas* axonemes devoid of outer or inner dynein arms. *J. Cell Biol.* 103:1895–1902.

27. Kamiya, R. 1982. Extrusion and rotation of the central-pair microtubules in detergent-treated *Chlamydomonas* flagella. *Prog. Clin. Biol. Res.* 80:169–173.

28. Mitchell, D. R., and M. Nakatsugawa. 2004. Bend propagation drives central pair rotation in *Chlamydomonas reinhardtii* flagella. *J. Cell Biol.* 166:709–715.

29. Sale, W. S., and P. Satir. 1977. Direction of active sliding of microtubules in *Tetrahymena* cilia. *Proc. Natl. Acad. Sci. USA.* 74:2045–2049.

30. Kamimura, S., and R. Kamiya. 1989. High-frequency, nanometer-scale vibration in ''quiescent'' flagellar axonemes. *Nature.* 340:476–478.

31. Kamimura, S., and R. Kamiya. 1992. High-frequency vibration in flagellar axonemes with amplitudes reflecting the size of tubulin. *J. Cell Biol.* 116:1443–1454.

32. Yagi, T., and R. Kamiya. 1995. Novel mode of hyper-oscillation in the paralyzed axoneme of a *Chlamydomonas* mutant lacking the central-pair microtubules. *Cell Motil. Cytoskeleton.* 31:207–214.

33. Johnson, K. A. 1983. The pathway of ATP hydrolysis by dynein. Kinetics of a presteady state phosphate burst. *J. Biol. Chem.* 258: 13825–13832.

34. Haward, J. 2001. Mechanics of Motor Proteins and the Cytoskeleton. Sinauer Associates, Sunderland, MA.

35. Kurachi, M., M. Hoshi, and H. Tashiro. 1995. Buckling of a single microtubule by optical trapping forces: direct measurement of microtubule rigidity. *Cell Motil. Cytoskeleton.* 30:221–228.

36. Felgner, H., R. Frank, and M. Schliwa. 1996. Flexural rigidity of microtubules measured with the use of optical tweezers. *J. Cell Sci.* 109:509–516.

37. Ishijima, S., and Y. Hiramoto. 1994. Flexural rigidity of echinoderm sperm flagella. *Cell Struct. Funct.* 19:349–362.

38. Hirakawa, E., H. Higuchi, and Y. Y. Toyoshima. 2000. Processive movement of single 22S dynein molecules occurs only at low ATP concentrations. *Proc. Natl. Acad. Sci. USA.* 97:2533–2537.

39. Sakakibara, H., H. Kojima, Y. Sakai, E. Katayama, and K. Oiwa. 1999. Inner-arm dynein c of *Chlamydomonas* flagella is a single-headed processive motor. *Nature.* 400:586–590.

40. Shingyoji, C., H. Higuchi, M. Yoshimura, E. Katayama, and T. Yanagida. 1998. Dynein arms are oscillating force generators. *Nature.* 393:711–714.

41. Takasone, T., S. Juodkazis, Y. Kawagishi, A. Yamaguchi, S. Matsuo, H. Sakakibara, H. Nakayama, and H. Misawa. 2002. Flexural rigidity of a single microtubule. *Jpn. J. Appl. Phys.* 41:3015–3019.

42. Sakakibara, H. M., Y. Kunioka, T. Yamada, and S. Kamimura. 2004. Diameter oscillation of axonemes in sea-urchin sperm flagella. *Biophys. J.* 86:346–352.